

## Supporting information

### Coupling Interconnected $\text{MoO}_3/\text{WO}_3$ Nanosheets within Graphene

### Framework as Highly Efficient Anode for Lithium-Ion Battery

Pengbo Wang, Zihua Cheng, Guiqin Lv\*, Liangti Qu\* and Yang Zhao\*

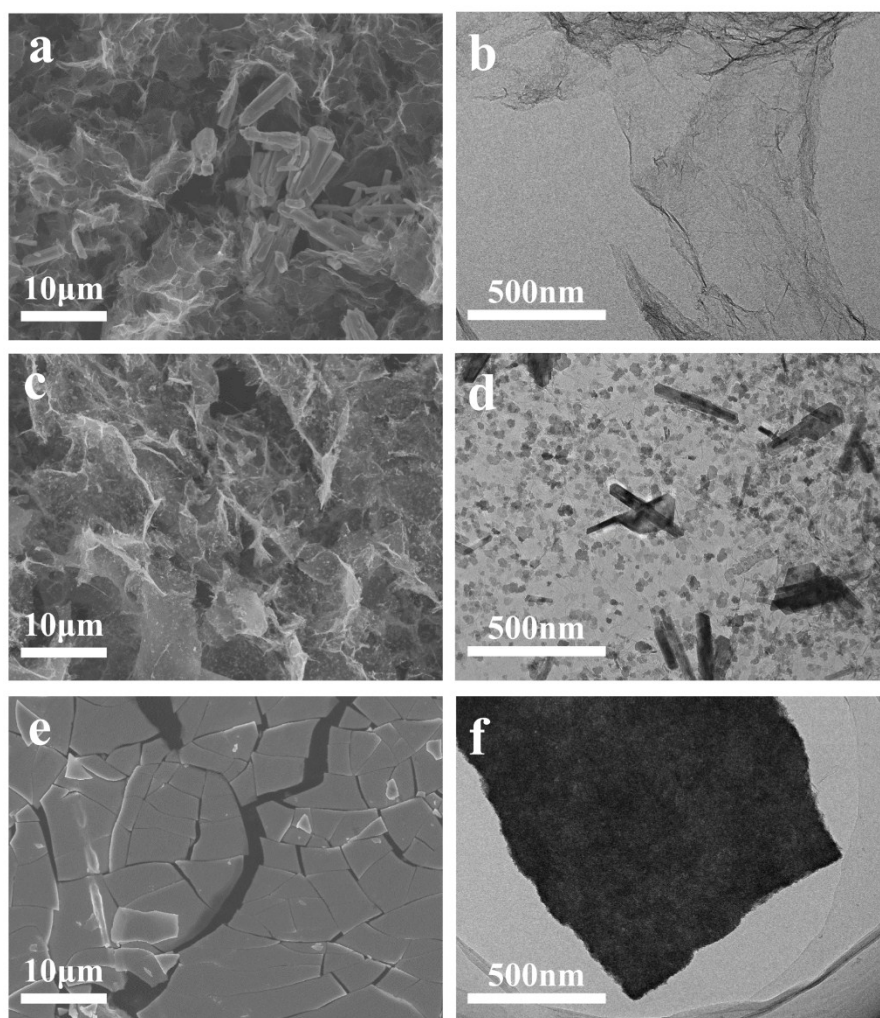


Fig. S1 The scanning (SEM) and transmission electron microscopy (TEM) images of the as-prepared (a, b)  $\text{MoO}_3$ -GF, (c, d)  $\text{WO}_3$ -GF and (e, f)  $\text{MoO}_3/\text{WO}_3$ .

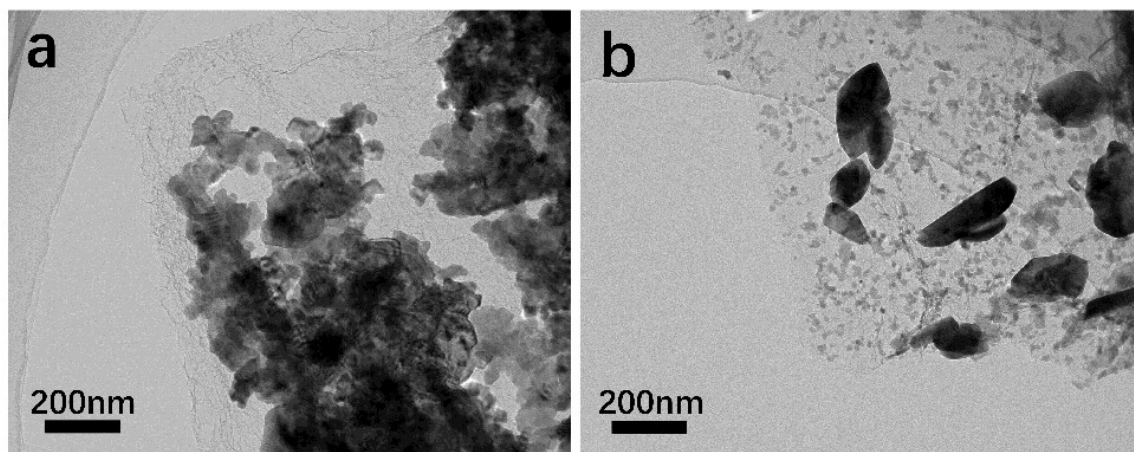


Fig. S2 The TEM images of the as-prepared (a) MoO<sub>3</sub>/WO<sub>3</sub>-GF-2/1 and (b) MoO<sub>3</sub>/WO<sub>3</sub>-GF-1/2, respectively.

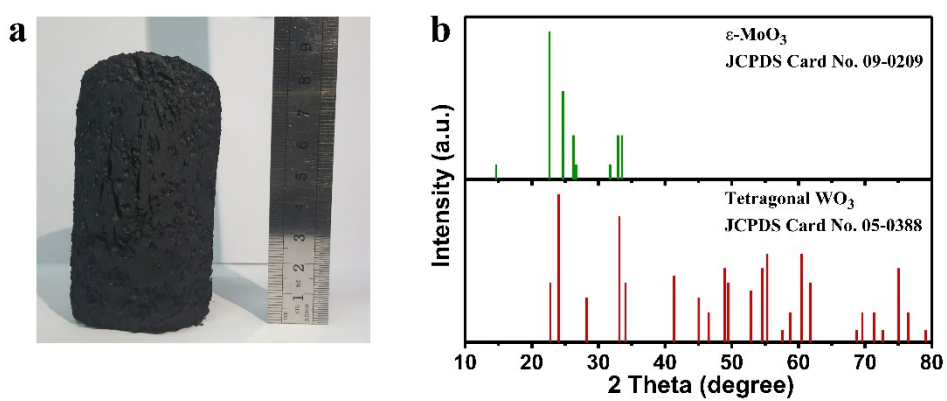


Fig. S3 (a) The digital image of MoO<sub>3</sub>/WO<sub>3</sub>-GF after hydrothermal treatment in a 300 mL Teflon-line autoclave. (b) Standard PDF card of ε-MoO<sub>3</sub> and tetragonal WO<sub>3</sub>.

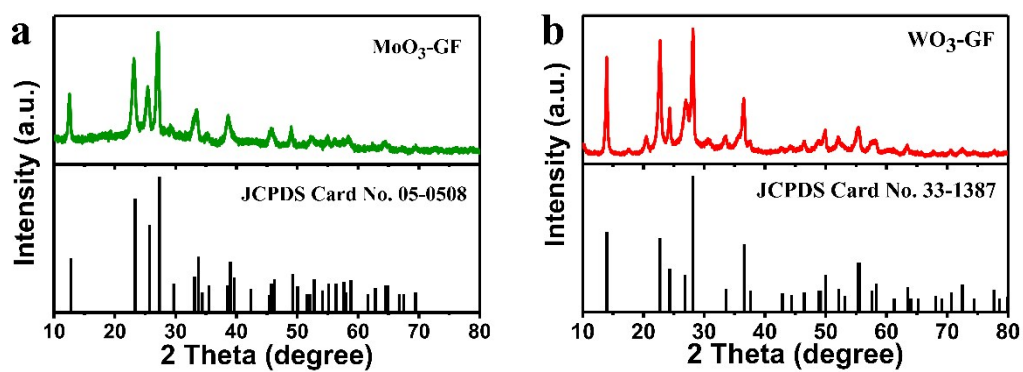


Fig. S4 X-ray diffraction (XRD) patterns of (a) MoO<sub>3</sub>-GF and (b) WO<sub>3</sub>-GF.

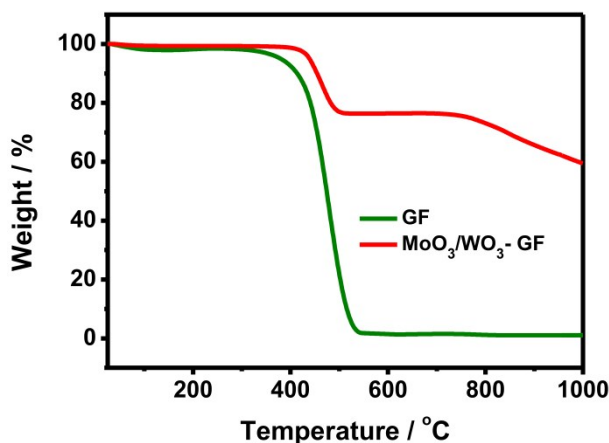


Fig. S5 The thermogravimetric analysis (TGA) curves of the MoO<sub>3</sub>/WO<sub>3</sub>-GF and GF in air from 25 to 1000 °C with a temperature ramping rate of 10 °C min<sup>-1</sup>.

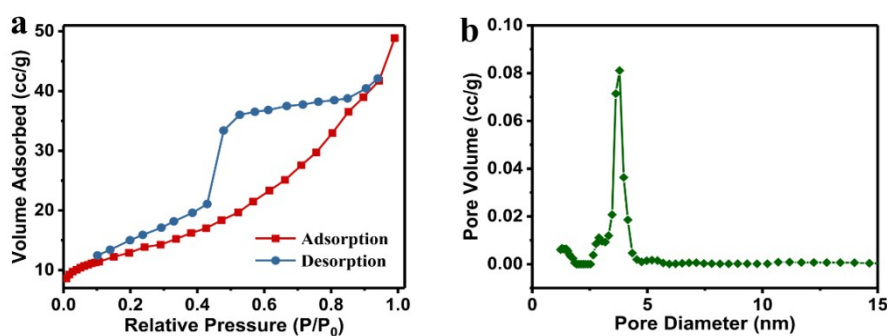


Fig. S6 The N<sub>2</sub> adsorption-desorption isotherm of (a) MoO<sub>3</sub>/WO<sub>3</sub>-GF and (b) the corresponding pore-size distribution.

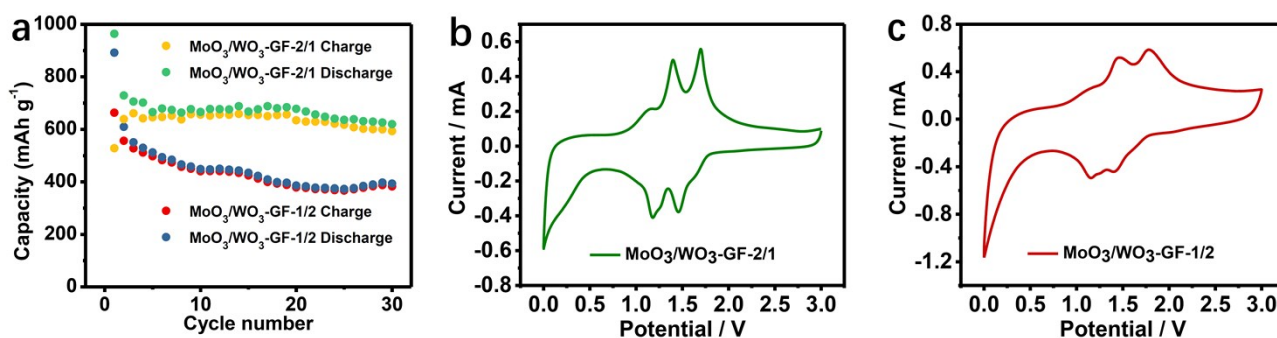


Fig. S7 Cycling performances of (a) MoO<sub>3</sub>/WO<sub>3</sub>-GF-2/1 and MoO<sub>3</sub>/WO<sub>3</sub>-GF-1/2 at 200 mA g<sup>-1</sup>, and the stable CV curves of (b) MoO<sub>3</sub>/WO<sub>3</sub>-GF-2/1 and (c) MoO<sub>3</sub>/WO<sub>3</sub>-GF-1/2 at a scan rate of 0.2 mV s<sup>-1</sup>, respectively.

As shown in Fig. S7a, the reversible discharge capacities of MoO<sub>3</sub>/WO<sub>3</sub>-GF-2/1 and MoO<sub>3</sub>/WO<sub>3</sub>-GF-1/2 are 619.8 and 393.1 mA h g<sup>-1</sup> at 200 mA g<sup>-1</sup> over 30 cycles, which are far lower than the as-prepared MoO<sub>3</sub>/WO<sub>3</sub>-GF material (Fig. 4b). The corresponding CV curves are shown in Fig. S7b and c. Both the MoO<sub>3</sub>/WO<sub>3</sub>-GF-2/1 and MoO<sub>3</sub>/WO<sub>3</sub>-GF-1/2 exhibit more significant redox peaks than MoO<sub>3</sub>/WO<sub>3</sub>-GF (Fig. 5a) at range of 1.0 ~ 2.0 V. This can be ascribed to that the large MoO<sub>3</sub>/WO<sub>3</sub> crystal size and disordered structures may lead to the enhanced of redox peaks, according to previous studies on morphology-dependent electrochemical performances.<sup>1,2</sup>

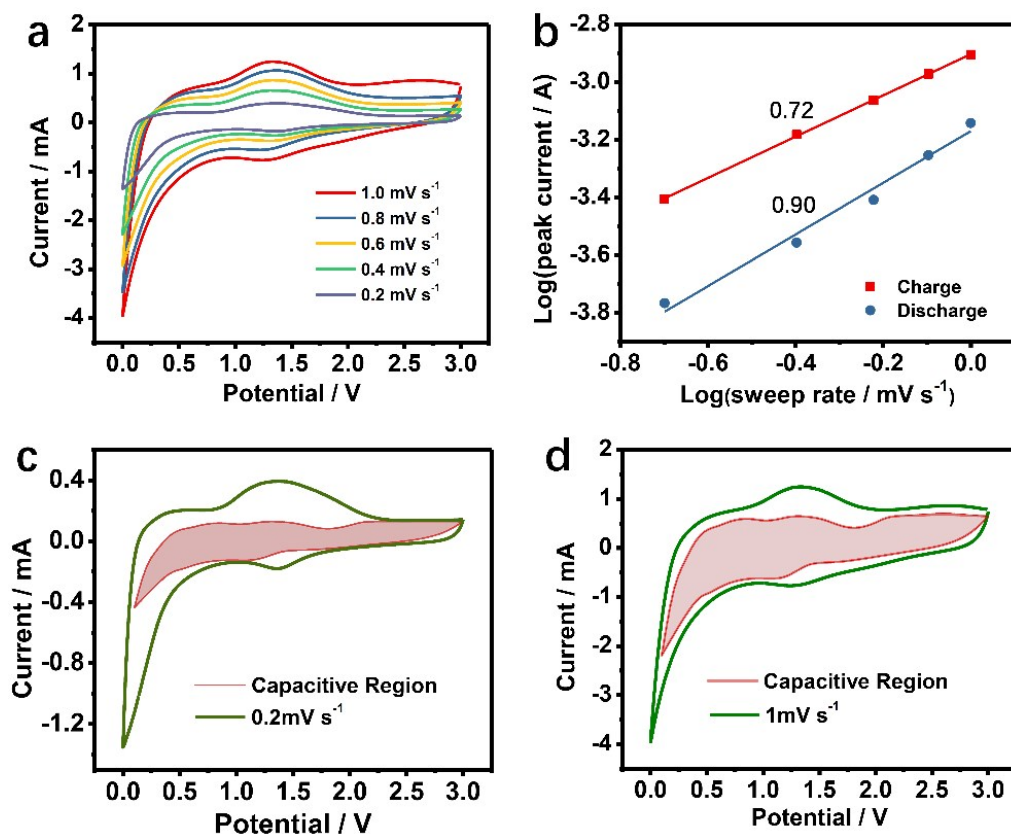


Fig. S8 (a) CV curves of MoO<sub>3</sub>/WO<sub>3</sub>-GF electrode with scan rate from 0.2 to 1 mV s<sup>-1</sup>. (b) The corresponding log (peak current, *i*) versus log (sweep rate, *v*) plots of charge and discharge peak current with scan rate from 0.2 to 1 mV s<sup>-1</sup>. (c) Voltammetric response at a scan rate of 0.2 mV s<sup>-1</sup> and (d) 1 mV s<sup>-1</sup> respectively. The capacitive contribution to the total current is shown by the shaded region.

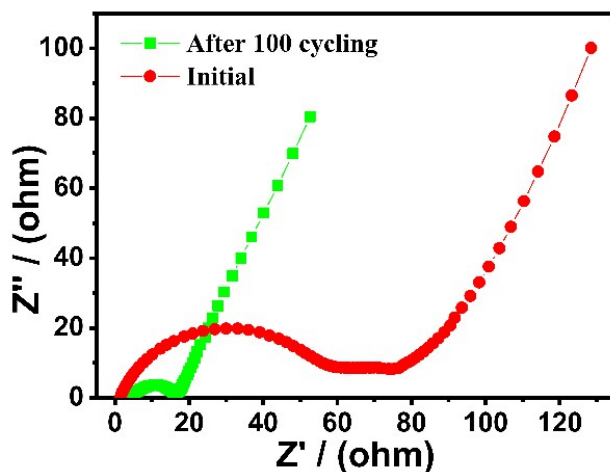


Fig. S9 Electrochemical impedance spectra (EIS) of MoO<sub>3</sub>/WO<sub>3</sub>-GF before and after cycling.

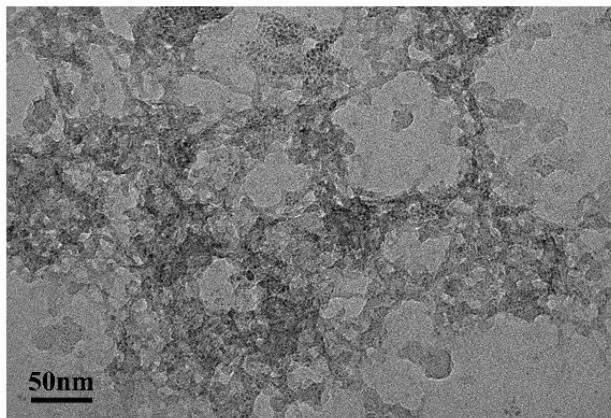


Fig. S10 The morphology of MoO<sub>3</sub>/WO<sub>3</sub>-GF after 100 cycles. This image gives the direct evidence of the structural stability of the material after cycling.

## Reference

- [1] Q. Xia, H. L. Zhao, Z.H. Du, J. Wang, T. H. Zhang, J. Wang and P. P. Lv, *J. Power Sources*, 2013, **226**, 107-111.
- [2] M. Okubo, E. Hosono, Jedeok Kim, M. Enomoto, N. Kojima, T. Kudo, H. S. Zhou and I. Honma, *J. Am. Chem. Soc.*, 2007, **129**, 7444-7452.